Supplementary Information: Experimental and computational study of solvent effects on one- and two-photon absorption spectra of chlorinated harmines

Dalibor Hršak,[‡a] Lotte Holmegaard,[‡a] Anton S. Poulsen,[a] Nanna H. List,[b] Jacob Kongsted,[b] M. Paula Denofrio,[c] Rosa Erra-Balsells,[d] Franco M. Cabrerizo,[*c] Ove Christiansen[*a] and Peter R. Ogilby[*a]

a Center for Oxygen Microscopy and Imaging, Aarhus University, Langelandsgade 140, 8000 Aarhus C, Denmark. Tel: +45 5152 6145, +45 8715 5927; E-mail: ove@chem.au.dk, progilby@chem.au.dk

b Department of Physics, Chemistry and Pharmacy, University of Southern Denmark, Campusvej 55, 5230 Odense M, Denmark.

c Instituto de Investigaciones Biotecnológicas, Instituto Tecnológico de Chascomús (IIB-INTECH), Universidad Nacional de San Martín (UNSAM), Consejo Nacional de Investigaciones, Científicas y Técnicas (CONICET), Intendente Marino Km 8.2, CC 164 (B7130IWA), Chascomús, Argentina. E-mail: fcabrerizo@intech.gov.ar

d CIHIDECAR–CONICET, Departamento de Química Orgánica, Facultad de Ciencias Exactas y Naturales, Universidad de Buenos Aires, Ciudad Universitaria, 1428 Buenos Aires, Argentina.

‡ These authors contributed equally to this work

S1 Computational procedure

S1.1 Creation of solvated systems

To include structural dynamical effects into the computational procedure, molecular dynamics (MD) simulations were performed on all six systems (three harmines in water and acetonitrile, respectively). The Maestro 9.3[1] graphical interface was utilized to setup 6 orthorhombic boxes of solvents around solutes, with distances of 15 Å away from the solute molecule in all six directions. The TIP3P water model[2] was used for aqueous solutions. The acetonitrile solvent model was designed using Maestro, following the procedure on the Schrödinger website. This procedure consisted of creating an array of 1024 MeCN molecules and a subsequent 1 ns MD simulation using the procedure described later. This resulted in a system with an equilibrated and homogeneous density and temperature, that can be used to create the solvation box around the chromophores.

In solution with pH = 4, the nitrogen atom next to the methyl group is protonated, giving a net charge of +1. To neutralize the solute–solvent systems, one Cl^- ion was added to each simulation box. This procedure resulted in three boxes of ∼1700 water molecules around the three observed chromophores and three boxes of ∼600 acetonitrile molecules.

S1.2 Molecular dynamics simulations

The MD simulations of these six systems were performed using the Desmond molecular simulations package[3] with the OPLS2005[4] force field for the solutes and MeCN.

We used general OPLS2005 parameters for the description of both the MeCN molecules and the chlorinated harmines.

Prior to the main simulation, a number of steps was performed for system equilibration. The first step was two minimizations; one with restraints of the solute molecules and one with no restraints. Thereafter two short simulations (12 ps) were performed at the temperature of 10K, using the Berendsen thermostat,[5] with constraints on the heavy atoms of the solute. The first simulation was performed within the NVT canoncal ensemble with a small timestep (0.001 ps). The next simulation was in the NPT canonical ensemble. Subsequently, two short simulation at temperature of 300K were performed with the Berendsen themostat and within the NPT ensemble. The first simulation lasted 12 ps and restraints were applied on heavy solute atoms, whereas the second simulation lasted 24 ps and had no restraints.

Finally, the main production simulations were initiated. The duration of these simulations was 2 ns, in the NPT canonical ensemble, at 300 K, using Nosé-Hoover chain thermostat[6,7] and isotropic Martyna-Tobias-Klein barostat.[8] The cutoff radius for long-range Coulomb interactions was 9 Å with smooth particle mesh Ewald scheme.[9,10] Snapshots of the trajectories were taken every 20 ps, producing 100 snapshots per simulation.

S1.3 QM/MM optimization and calculation of embedding potentials

The solute–solvent configurations used in the OPA and TPA property calculations were generated by performing point-charge electrostatic embedding QM/MM ge-

ometry optimizations of the solutes at the B3LYP[11]/cc-pVTZ[12]/OPLS2005[4] level of theory using the program Qsite.[13] The solvent molecules were kept fixed at the positions derived from the MD simulation. The solvent embedding potentials (referred to as M2P2) that, in addition to permanent electric multipole moments up to quadrupoles, consist of anisotropic electric dipole–dipole polarizabilities distributed at the atomic centers were derived according to the localized properties (LoProp) approach[14] implemented in the Molcas program,[15,16] employing the B3LYP exchange–correlation functional and the 6-31+G*[17–19] basis set. The generation of the embedding potentials was facilitated by the PE Assistant Script (PEAS).[20] The basis set was recontracted to an atomic natural orbital type basis as required for the LoProp approach.

S1.4 PE calculations and data analysis

The M2P2 embedding potentials were used in the PE-TDDFT[21,22] and PERI-CC2[23] property calculations of the solute–solvent systems. PE-TDDFT calculations were performed for 100 snapshots and PERI-CC2 calculations only for the first 50 snapshots, due to the higher computational cost of the PERI-CC2 calculations. All the calculations were performed with the approximation of electric-dipolar coupling between initial and final states.

The result of these calculations is a set of OPA excitation energies (ω), oscillator strengths (f) and two-photon transition strengths (δ^{TPA}). Their time fluctuations from the above described procedure are graphically depicted in figure S1.

Posterior data analysis included convolution of spectra using a line-shape func-

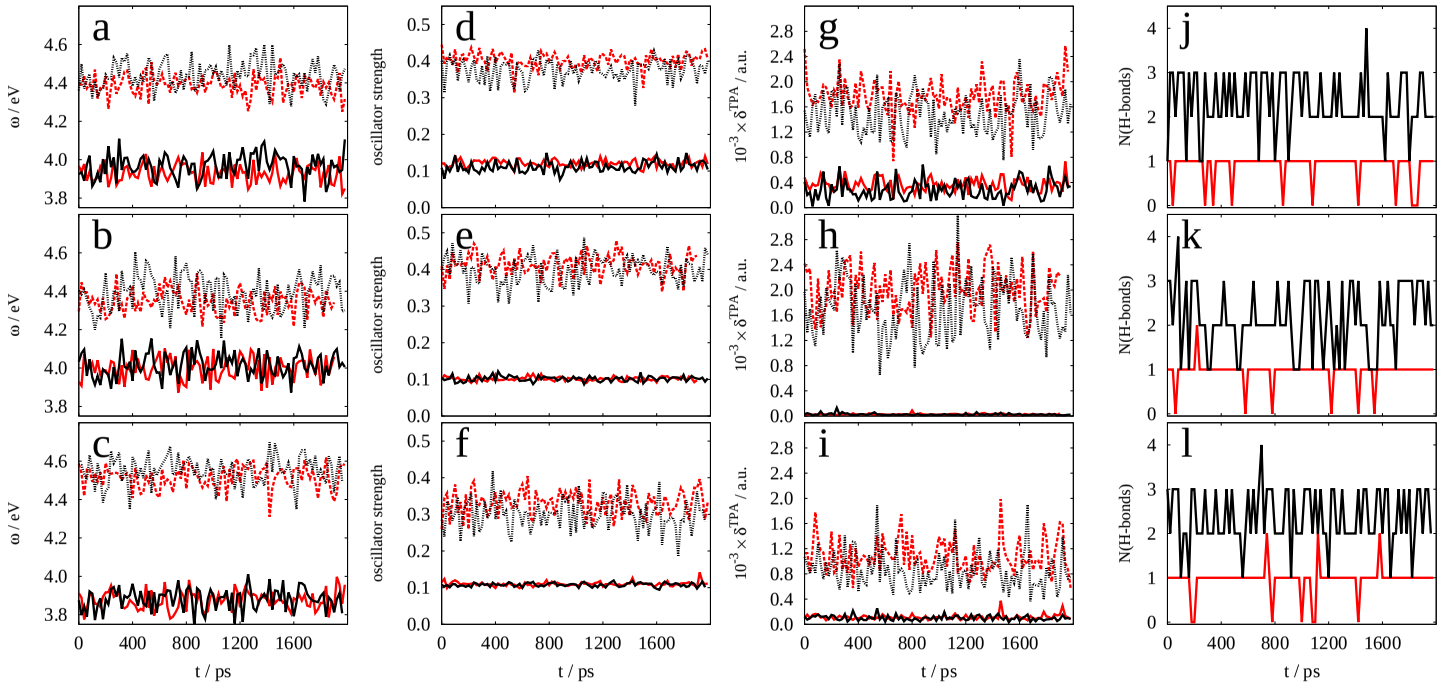

Figure S1: Time-fluctuations of the excitation energies (a-c), oscillator strengths (d-f) and TPA probabilities (g-i) of 6-Cl-Ha (a, d, g, j), 8-Cl-Ha (b, e, h, k), 6,8-diCl-Ha (c, f, i, l) for the first two excited states in water (black lines) and acetonitrile (red lines) obtained from PE-TDDFT calculations. The first excited state is depicted with solid lines and the second excited state with dashed lines. The number of solute–solvent hydrogen bonds in time is shown in graphs j-l.

Table S1: Pearson's correlation coefficients (r) of oscillator strengths (f) and two-photon transition probabilities (δ^{TPA}) with their respective excitation energies (ω) for the first and second excited state in solutions. The computational method is PE-TDDFT.

molecule	solvent	$r\left(f_1, \omega_1\right)$	$r\left(f_2, \omega_2\right)$	$r\left(\delta_1^{\mathrm{TPA}}, \omega_1\right)$	$r\left(\delta_2^{\mathrm{TPA}}, \omega_2\right)$
6-Cl-Ha	MeCN	-0.21	-0.52	-0.41	-0.78
	H_2O	0.04	-0.67	-0.29	-0.80
8-Cl-Ha	MeCN	0.30	-0.56	-0.32	-0.90
	H_2O	0.40	-0.76	-0.12	-0.94
6,8-diCl-Ha	MeCN	0.43	-0.48	-0.18	-0.88
	H_2O	0.57	-0.70	-0.55	-0.90

tion. The oscillator strengths from OPA calculations were convoluted using a Lorentzian-shape function of frequency of the form:

$$I\left(\omega\right) = \frac{1}{\pi} \sum_i \frac{\frac{1}{2}\mathrm{FWHM}}{\left(\omega - \omega_i\right)^2 + \left(\frac{1}{2}\mathrm{FWHM}\right)^2} f_i, \tag{S1}$$

where index i runs over all excited states and ω_i and f_i are the associated excitation energies and oscillator strengths, respectively. FWHM denotes full-width-at-half-maximum and is set to 0.35 eV. In order to obtain a spectrum in the scale of molar extinction coefficients, comparable with the experimental spectrum, the final spectrum was calculated using the following formula that describes the dependence of the molar extinction coefficient on the frequency[24]

$$\varepsilon\left(\omega\right) = \frac{N_A e^2}{4 m_e c^2 \epsilon_0 \ln 10} I\left(\omega\right) \tag{S2}$$

where N_A is the Avogadro's number, e is the elementary charge, m_e is the mass of

electron and c the speed of light.

The TPA spectra were simulated by means of convolution of the TPA probabilities into a Lorentzian function of frequency of the form

$$I\left(2\omega\right)=\frac{1}{\pi}\sum_{i}\frac{\frac{1}{2}\mathrm{FWHM}}{\left(2\omega-\omega_{i}\right)^{2}+\left(\frac{1}{2}\mathrm{FWHM}\right)^{2}}\delta_{i}^{\mathrm{TPA}}, \tag{S3}$$

and the final TPA cross section is calculated as

$$\sigma^{\mathrm{TPA}}\left(\omega\right)=\frac{4\pi^{3}\alpha a_{0}^{5}\omega^{2}}{c}I\left(2\omega\right). \tag{S4}$$

The FWHM is set to 0.2 eV (converted to atomic units) for the two-photon spectra. All the quantities in the Eqs. (S1) – (S4) are given in atomic units except the factor in front of the lineshape function in Eq. (S4), which is given in cgs units. The expression for conversion from cgs to Göppert-Mayer (GM) units for the latter equation is $1\mathrm{GM}=10^{-50}cm^{4}\cdot s\cdot\mathrm{photon}^{-1}$.

The dependence of the oscillator strengths and TPA transition probabilities on the excitation energies throughout the set of 100 snapshots per solvated system was evaluated using the Pearson's correlation coefficient.[25] The equation for the correlation coefficient r between two variables x and y is

$$r(x,y)=\frac{\sum_{i=1}^{N}\left(x_{i}-\bar{x}\right)\left(y_{i}-\bar{y}\right)}{\sqrt{\sum_{i=1}^{N}\left(x_{i}-\bar{x}\right)^{2}}\sqrt{\sum_{i=1}^{N}\left(y_{i}-\bar{y}\right)^{2}}}, \tag{S5}$$

where x_i and y_i are elements of two data sets of the size N, and $\bar{x}$ and $\bar{y}$ are the mean values of these two sets. r can have values between -1 and 1. A value of $r = 1$ means there is a perfect linear positive correlation, while $r = -1$ means negative correlation between the sets x and y. Values near zero mean there is no correlation. The coefficients are listed in Table S1.

References

1 *Maestro, version 9.3, Schrödinger, LLC, New York, NY*, 2012.

2 W. L. Jorgensen and J. D. Madura, *J. Am. Chem. Soc.*, 1983, **105**, 1407–1413.

3 *Desmond Molecular Dynamics System, Copyright 2004-2012, D. E. Shaw Research, provenance 3.1.51.1*.

4 J. L. Banks, H. S. Beard, Y. Cao, A. E. Cho, W. Damm, R. Farid, A. K. Felts, T. A. Halgren, D. T. Mainz, J. R. Maple, R. Murphy, D. M. Philipp, M. P. Repasky, L. Y. Zhang, B. J. Berne, R. A. Friesner, E. Gallicchio and R. M. Levy, *J. Comput. Chem.*, 2005, **26**, 1752–1780.

5 H. J. C. Berendsen, J. P. M. Postma, W. F. van Gunsteren, A. DiNola and J. R. Haak, *J. Chem. Phys.*, 1984, **81**, 3684–3690.

6 S. Nosé, *J. Chem. Phys.*, 1984, **81**, 511–519.

7 W. G. Hoover, *Phys. Rev. A*, 1985, **31**, 1695–1697.

8 G. J. Martyna, D. J. Tobias and M. L. Klein, *J. Chem. Phys.*, 1994, **101**, 4177–4189.

9 U. Essmann, L. Perera, M. L. Berkowitz, T. Darden, H. Lee and L. G. Pedersen, *J. Chem. Phys.*, 1995, **103**, 8577–8593.

10 T. Darden, D. York and L. Pedersen, *J. Chem. Phys.*, 1993, **98**, 10089–10092.

11 P. J. Stephens, F. J. Devlin, C. F. Chabalowski and M. J. Frisch, *J. Phys. Chem.*, 1994, **98**, 11623–11627.

12 T. H. Dunning, *J. Chem. Phys.*, 1989, **90**, 1007–1023.

13 *QSite, version 5.8, Schrödinger, LLC, New York, NY*, Schrödinger, LLC, New York, NY, 2012.

14 L. Gagliardi, R. Lindh and G. Karlström, *J. Chem. Phys.*, 2004, **121**, 4494–4500.

15 G. Karlström, R. Lindh, P.-Å. Malmqvist, B. O. Roos, U. Ryde, V. Veryazov, P.-O. Widmark, M. Cossi, B. Schimmelpfennig, P. Neogrady and L. Seijo, *Comput. Mater. Sci.*, 2003, **28**, 222–239.

16 F. Aquilante, L. De Vico, N. Ferré, G. Ghigo, P.-Å. Malmqvist, P. Neogrády, T. B. Pedersen, M. Pitoňák, M. Reiher, B. O. Roos, L. Serrano-Andrés, M. Urban, V. Veryazov and R. Lindh, *J. Comput. Chem.*, 2010, **31**, 224–247.

17 W. J. Hehre, R. Ditchfield and J. A. Pople, *J. Chem. Phys.*, 1972, **56**, 2257–2261.

18 P. Hariharan and J. Pople, *Theor. Chim. Acta*, 1973, **28**, 213–222.

19 T. Clark, J. Chandrasekhar, G. W. Spitznagel and P. V. R. Schleyer, *J. Comput. Chem.*, 1983, **4**, 294–301.

20 J. M. H. Olsen, *PhD thesis*, University of Southern Denmark, Odense, Denmark, 2012.

21 J. M. H. Olsen, K. Aidas and J. Kongsted, *J. Chem. Theory Comput.*, 2010, **6**, 3721–3734.

22 J. M. H. Olsen and J. Kongsted, *Advances in Quantum Chemistry*, 2011, **61**, 107 – 143.

23 T. Schwabe, K. Sneskov, J. M. H. Olsen, J. Kongsted, O. Christiansen and C. Hättig, *J. Chem. Theory Comput.*, 2012, **8**, 3274–3283.

24 M. Sauer, J. Hofkens and J. Enderlein, in *Basic Principles of Fluorescence Spectroscopy*, Wiley-VCH Verlag GmbH and Co. KGaA, 2011, pp. 1–30.

25 K. Pearson, *Proc. R. Soc.*, 1895, **58**, 240–242.